Naval Research Laboratory

Washington, DC 20375-5320

NRL/MR/6790--98-7998

Increase in Rosseland Mean Opacity for Inertial Fusion Hohlraum Walls

D. COLOMBANT

Beam Physics Branch
Plasma Physics Division

M. KLAPISCH
A. BAR-SHALOM

ARTEP, Inc.
Columbia, MD

March 23, 1998

REPORT DOCUMENTATION PAGE

Form Approved
OMB No. 0704-0188

1. AGENCY USE ONLY (*Leave Blank*)	2. REPORT DATE	3. REPORT TYPE AND DATES COVERED
	March 23, 1998	Interim

4. TITLE AND SUBTITLE

Increase in Rosseland Mean Opacity for Inertial Fusion Hohlraum Walls

5. FUNDING NUMBERS

6. AUTHOR(S)

D. Colombant, M. Klapisch,* and A. Bar-Shalom*†

7. PERFORMING ORGANIZATION NAME(S) AND ADDRESS(ES)

Naval Research Laboratory
Washington, DC 20375-5320

8. PERFORMING ORGANIZATION REPORT NUMBER

NRL/MR/6790--98-7998

9. SPONSORING/MONITORING AGENCY NAME(S) AND ADDRESS(ES)

U.S. Department of Energy
Washington, DC 20585

10. SPONSORING/MONITORING AGENCY REPORT NUMBER

11. SUPPLEMENTARY NOTES

*ARTEP, Inc., Columbia, MD 21045
†Permanent Address: NRCN, P.O. Box 9001, Beer Sheva, Israel

12a. DISTRIBUTION/AVAILABILITY STATEMENT

Approved for public release; distribution unlimited.

12b. DISTRIBUTION CODE

13. ABSTRACT (*Maximum 200 words*)

The Rosseland mean opacity of hohlraum gold walls can be increased by filling in the low absorption gaps in the gold spectrum with one or more additional elements. Using our opacity code STA, we investigated various mixtures. A combination of gold and copper, or nickel, is equivalent or better than the previously proposed gold and gadolinium mixture, and is much easier to fabricate. Other more elaborate mixtures yield even higher opacities.

Our simulations are in good agreement with experiment. At the temperatures and densities of interest, non-LTE corrections are minor, of order 10%, and not significant in view of the experimental accuracy.

14. SUBJECT TERMS

Rosseland opacity
Hohlraum wall
Opacity of mixtures

15. NUMBER OF PAGES

27

16. PRICE CODE

17. SECURITY CLASSIFICATION OF REPORT	18. SECURITY CLASSIFICATION OF THIS PAGE	19. SECURITY CLASSIFICATION OF ABSTRACT	20. LIMITATION OF ABSTRACT
UNCLASSIFIED	UNCLASSIFIED	UNCLASSIFIED	UL

NSN 7540-01-280-5500

Standard Form 298 (Rev. 2-89)
Prescribed by ANSI Std 239-18
298-102

CONTENTS

INCREASE IN ROSSELAND MEAN OPACITY FOR INERTIAL FUSION HOHLRAUM WALLS

1.Introduction

The hohlraum walls for indirect laser fusion targets have typically been constructed of a single high-Z material such as gold. High-Z materials have a high opacity over a broad range of the x-ray spectrum. X-rays are produced by the interaction of the laser beams with the gold walls. In turn, part of those x-rays heat and ablate the wall. Higher opacities reduce the x-ray energy losses to the wall and maximize the coupling efficiency of the radiation to the fuel pellet. However the gold absorption spectrum at the hohlraum temperature, like that of any other element, is not constant over frequency: it has peaks and minima, and the opacity is significantly lower in some frequency regions.

In a recently published paper [1], Orzechowski *et al.* have shown that it is possible to increase the opacity of the hohlraum walls by adding other materials to the gold. The authors of [1] mixed gadolinium (Gd) with gold, and showed experimentally an increase of more than 40% in the Rosseland mean opacity at a temperature of 250 eV and a density of 1 g/cm^3. Because Au and Gd do not mix well, they resorted to an elaborate technique of multilayering. Their experimental results agreed with their calculations, using their opacity model XSN[2].

The concept of increasing the Rosseland mean opacity is easy to explain. The absorption spectrum displays saw-tooth features which are characteristic of the photoionization of the various atomic shells, in addition to the bound-bound transitions. The Rosseland mean opacity is defined as

$$\frac{1}{\kappa_R} = \frac{\int_0^\infty \kappa_\nu^{-1} \left(\partial B_\nu / \partial T\right) d\nu}{\int_0^\infty \left(\partial B_\nu / \partial T\right) d\nu} \qquad (1)$$

where T is the temperature, B_ν is the Planck function, κ_ν is the frequency-dependent opacity and κ_R is the mean opacity. The peak of the weight function $\partial B_\nu / \partial T$ lies around 1 keV for a temperature of 250 eV. Because the opacity κ_ν enters this expression

Manuscript approved November 3, 1997.

as an inverse, the minima dominate the value of the inverse mean. Many medium and high Z elements have absorption peaks that will fill up some of the minima in the spectrum for gold, as shown in Fig.1 of ref.[1]. Therefore the mixture will increase the mean opacity. We have assumed here that matter is in local thermodynamic equilibrium (LTE), a reasonably accurate approximation that we will discuss later in the paper.

The purpose of this work is multi-fold: *i*) search for elements which increase the opacity as much as Gd and which would mix more easily with gold; *ii*) study the opacity of that mixture for a range in parameter space which spans the time-evolution of the hohlraum; *iii*) attempt to increase the opacity even more by adding more elements; *iv*) compare our numerical results with the experimental results already published. The following sections describe the computational methodology, provide the absorption spectra of various elements and mixtures and their variation in temperature-density space, and estimate non-LTE effects.

2. Computational codes and methodology

We utilize our LTE opacity code STA for this problem[3-6]. A previous version of the STA code has already been compared with absorption measurements, and there was good agreement, both on frequency-dependent opacities[7, 8] and Rosseland mean[9]. For most of the elements mentioned below, frequency-dependent opacities were computed at a temperature of 250 eV, typical of the high-intensity regime for the proposed NIF laser, and at a few densities around $1 g/cm^3$, again typical of the higher-density portion of the wall that provides the useful opacity. The resulting databases were then post-processed by our program MIX, which computes group-average opacities. This program first computes effective densities for each element of a mixture to enforce the equality of chemical potentials as a condition for equilibrium. These effective densities are then used as look-up entries for spectra retrieval in the databases generated by the STA code. If necessary, MIX will interpolate between neighboring tabular densities. MIX is versatile and can utilize different resolutions in different spectral ranges, so that we

could verify the convergence and the numerical accuracy of the Rosseland mean opacity computations. Most of the following computations used a resolution of 16eV; some were verified with a resolution of 2eV. The mean opacities changed by less than 0.5% for the elements considered in this paper.

3. Opacity results for Au-Cu alloy

First of all, we look at opacities at a fixed temperature T=250eV and density $\rho=1 g/cm^3$, which were determined to be the prevailing parameters for the hohlraum in ref. [1].

Almost any mixture of gold with another material will have a higher opacity than pure gold. Many medium and high-Z elements would be a good choice because they have absorption peaks that are near the troughs in the gold spectrum. These peak positions vary with Z, so elements that are very close to gold in the periodic table overlap with gold and are not useful. However, if one wants to optimize the mean opacity for a very specific temperature, or as we shall see later for a range of temperatures not too broad - say a factor of two-, then one should look for elements whose absorption peaks *a*) fill the gaps in the gold spectrum and *b*) are located near the maximum of the weight function, around four times the temperature.

We have computed the opacities of many elements at the above temperature and density. From the many elements we looked at and which will be reported below, we concentrate on the copper alloy with gold because its Rosseland mean opacity is comparable to that of the Au-Gd mixture described in ref.[1] and because of its much better availability and much easier fabrication. The following results apply equally well to a nickel-gold alloy.

A comparison between the Au-Cu and Au-Ni alloys and the Au-Gd compound is shown in Fig.1 where the Rosseland mean opacity is plotted for the mixtures as a function of the fraction of gold. The opacity distribution for Au-Gd is quite symmetrical

with respect to the 50-50 mixture, whereas it is tilted towards a lower concentration of gold for the Au-Cu and Au-Ni alloys.

For this point in temperature-density space, the maximum Rosseland mean is slightly larger for the Au-Cu and Au-Ni alloys. However it is important to check if this advantage holds for a wider region of parameter space, representative of the evolution of the conditions at the hohlraum wall. With this purpose in mind, we looked at opacities of the Au-Cu alloy over a range of temperatures varying from 150 eV to 300 eV and densities going from 0.4 g/cm^3 to 3.3 g/cm^3. We looked at many cases where we varied the temperature and adjusted the density so that the product of the two was kept constant, starting from the initial point of T=250eV and ρ=1g/cm^3. We then divided the density by 2 , then multiplied it by 2, over the same range of temperatures. We also kept the density constant, varying the temperature only. All these variations produced similar results which can be shown typically in Figs. 2 and 3. In Fig. 2, we show the Rosseland mean for a 30%Au-70%Cu alloy compared to that of a 70%Au-30%Gd combination and that of pure gold for temperatures varying from 150 eV to 300 eV while keeping the density constant. These proportions are nearly optimal on average. In Fig. 3, we show the same quantity for a 30%Au-70%Cu alloy, a 50%Au-50%Gd mixture and pure gold, as a function of density for a constant temperature of 250eV. From these figures, we note that the opacities and their trends do not depend very much on the concentrations of copper or gadolinium. This is consistent with Fig. 1, showing that the maxima as a function of concentration are rather broad.

These graphs show that the Rosseland means are very similar for both mixtures as a function of temperature, in general slightly higher for the copper alloy at temperatures up to about 250 eV, and slightly higher for the gadolinium mix above that value. The opacities for the mixtures are better than that for pure gold by 6 to 10% at 150 eV and by up to 45% at 300 eV. So the gain in opacity becomes more important as the temperature

increases. This shows that more attention should be brought to this topic as the hohlraums become hotter.

We show in Figs. 4 and 5, the Cu and Gd absorption spectra at 150 and 300 eV respectively for a density of 1g/cm^3, along with the corresponding Rosseland weight function $\partial B_\nu / \partial T$.

It can be seen on these graphs that the position of the absorption peaks near 1keV varies only slightly with temperature. The reason is that these transitions involve deep shells (n=2→3 for Cu and n=3→4 for Gd), that are not very much dependent on the ion stage. The average charge Z^* for these elements at these temperatures can be found in Table I. However, the importance of these peaks decrease with the shifting of $\partial B_\nu / \partial T$ towards lower energies as the temperature goes down. At T=300eV, the peak contributes 2/3 of the integral in the numerator of eq. 1 for Cu and 1/2 for Gd. At T=150 eV, on the other hand, these contributions are only 1/2 and 1/7 respectively. The remainder of the opacity comes from the spectral features in the 100-500eV range. These transitions correspond to optical shells (n=3→4 for Cu and n=4→5 for Gd), whose energy is more dependent on the ion stage, and therefore on the temperature. There are also Δn=0 (4→4) transitions for both elements around 100-120 eV, at both temperatures. In the last two types of transitions, the intensity goes down with temperature, because of the shift in the ion distribution. The interplay between the position of $\partial B_\nu / \partial T$ and the intensity and energy of the transitions is thus a natural mechanism accounting for the smoothness of the Rosseland mean as a function of temperature and density. This mechanism accounts also probably for the fact that the slopes $\partial \kappa_R / \partial T$ and $\partial \kappa_R / \partial \rho$ of the two mixtures and of pure gold in Fig. 2 and Fig. 3 are remarkably similar. We will therefore hypothesize for the next section that if the elements we study have the same kind of spectra in this range of T and ρ, their temperature and density dependence $\partial \kappa_R / \partial T$, $\partial \kappa_R / \partial \rho$ will be very close. Thus the performance of various mixtures obtained for an appropriate single T-ρ point can probably apply to a broader region of

temperature and density, relevant to the evolution of density and temperature at the hohlraum walls.

4. Absorption spectra for various elements and mixtures

Now going back to the single point in parameter space defined by T=250eV and ρ=1g/cm^3, we will show that larger values of Rosseland means can be achieved, albeit for less practical mixtures. In this section, we do not bother to check whether these mixtures are feasible or not from the point of view of their chemical and physical properties. Our point is to find an empirical upper bound to the Rosseland mean.

We have computed the opacities of many elements, and we chose Ag, Cs, Nd, Sn, Co, Mn, Se besides Gd,Cu, and Ni because they all display an absorption peak near 1 keV, as shown in Table II, column 3. The conclusions of the preceding section also apply to these elements. Because cesium is liquid at room temperature, we replaced it by its iodide (CsI) which has almost the same spectrum as Cs since iodine is very close to cesium in the periodic table of elements.

Let us note first that the Rosseland mean opacity we calculate for pure gold is slightly larger than in ref.[1]. There the value of 1500 cm^2/g was obtained with the XSN model, and 823 cm^2/g with another average-atom model. The STA value is 1620 cm^2/g. The Rosseland mean for each of the other elements is shown in the second column of Table II. Note also that the pure elements have a wide range of opacity values, ranging from 657 cm^2/g for Se to 2056 cm^2/g for CsI. The maximum values for the Rosseland mean opacities of the mixtures obtained by mixing gold with each of the ten "elements" Ag, Co , CsI , Cu, Gd, Mn, Nd, Ni, Se, and Sn appear on column 4 of Table II.

Since the opacity for mixtures of two elements increases over that of pure elements, it is natural to examine three elements, and then four, and so on. To search this multi-dimensional space we took the fractions of two elements corresponding to their maximum opacity, and then progressively added a third element. Starting from Au-CsI

and Au-Co mixtures, because of the location of their absorption peaks near 1 keV, we added respectively Gd or Ag because these elements have peaks which are respectively higher and lower than 1 keV. The maximum mean opacities obtained at a temperature of 250 eV and a total mass density of $1 g/cm^3$ were 2715 cm^2/g for an Au-CsI-Gd mixture, 2605 cm^2/g for Au-CsI-Ag, 2670 cm^2/g for an Au-CsI-Nd, 2592 cm^2/g for the Au-CsI-Sn, but only 2382 cm^2/g for Au-Gd-Ag. We examined the same type of mixture with medium-Z elements, including Au-Co-Cu for which we got 2365 cm^2/g, and Au-Co-Mn with 2156 cm^2/g. We also tried to mix the higher Z elements with the medium Z ones, but without any striking success. In general, adding a third element increases the opacity only slightly. Physically, the second element fills up most of the gaps in the absorption spectrum whereas a third element can only fill the less important remaining ones. The "best" opacity with three elements was the mixture of 24% Au, 56% CsI and 20% Gd mentioned above. This trend is confirmed by the addition of a fourth element. The best overall result was obtained with a mixture of 15% Au, 25% Gd, 35% CsI and 25% Ag, with 2844 cm^2/g. The spectrum for the latter normalized mixture, without the gold, (29.5% Gd, 41% CsI and 29.5% Ag) is shown in Fig. 6 . The central absorption peak falls at 967 eV –due to CsI–, whereas the maximum of $\partial B_V / \partial T$ is at 983 eV. We find in general that it is the details of the spectra which control these opacity calculations and that, without these details, it is not possible to accurately calculate the combined opacities. To improve upon this Au+CsI+Gd+Ag mixture, one would have to find other elements whose combination of absorption peaks at this temperature fills up most of the gaps around the maximum of $\partial B_V / \partial T$.

Our best result has an increase in opacity of 76% over pure gold. No element will fill all the gaps in the gold absorption spectrum in a perfect fashion, and once the gaps are roughly filled, improvements come only in smaller amounts. Because the purpose of this section was not to find a practical wall compound with the best possible opacity

properties, studying its opacity variation with temperature and density was not repeated here. It is expected to behave in the way outlined at the end of section 3.

5. Non-LTE effects

We use Busquet's model [11, 12] to estimate non-LTE effects. Non-LTE is the most natural state of any experimental radiating plasma since LTE assumes that all radiation is reabsorbed by the plasma and does not escape it. We shall discuss these effects only for the single point of temperature and density previously mentioned. Busquet's model is based upon the insight that ion populations in the non-LTE regime should follow roughly a Saha-Boltzmann distribution at a different temperature, T_Z , called the ionization temperature. Very simply, T_Z is defined so that the average ion charge at T_Z in LTE is the same as the average charge at T_e in non-LTE. One can then use LTE-based opacities to obtain non-LTE opacities. This very powerful result has been checked by detailed collisional-radiative models in the optically thin case [13-15].

To estimate T_Z for this problem, we applied the algorithm described in ref [11]. For an optically thin plasma at T_e= 250 eV and $\rho = 1 g/cm^3$, T_Z = 226 eV. Introducing a radiation temperature of T_R =225 eV[1, 16], we computed a corrected T_Z = 243 eV, including radiation effects. The decrease in temperature was less than 3% with respect to the original T_e. At this temperature, the Rosseland mean opacity for pure Au is 1820 cm^2/g, with the other elements mentioned in the previous section shown in Table III, column 2. The opacities all decrease with increasing temperature, as was seen previously in Fig. 2, with the largest change occuring for gold. Over the range 150-300 eV, a doubling in temperature leads to a factor of 2.9 change in the gold opacity, at constant density. This is a larger change than predicted by the scaling law given in ref. [1] based on the XSN model. We looked at the scaling of opacity for Gd and Cu over that same range of temperature. For Gd, it changed by a factor of 2.5 and by a factor of 2.0 for Cu. So, it seems that a slight atomic number dependence could be included in the previously reported scaling law[1].

6. Comparison with experiment

Figure 7 shows the opacities for a Au-Gd mixture at T_Z =243 eV, along with the results from ref. [1], including the XSN predictions at 250 eV and the experimental data. The measured opacities are normalized to the XSN opacity of pure gold. The STA(LTE) results for pure gold are within the error bars of the experimental results. For the measured Au+Gd mixtures, the STA(LTE) results are lower than the XSN opacities and closer to the experimental values.

The non-LTE effects with an effective temperature of T_Z =243eV shift the results well within the error bars. However, one should exercise caution before evaluating the importance of non-LTE effects at this density of 1 g/cm^3. The relative difference between T_Z and T_e is less than 3%, and measurements of the Rosseland mean opacity are approximate. In addition, the measurements have assumed the temperature to be constant, so it is quite difficult to come up with any firm conclusion as far as this comparison between calculations and experiment is concerned. In any case, a decrease in the effective temperature seems to improve the agreement with experiment.

7. Conclusions

Concerning the maximum obtainable increase in opacity, it has been shown that a well chosen mixture of four elements allowed us to increase the opacity by 75% at 250 eV and 1g/cm^3 with respect to pure gold. However, this particular mixture will probably not be feasible for a variety of reasons, and it has to be considered as an upper bound on the opacity.

We also found that a copper alloy with gold could provide a wall with similar or better characteristics than one made up of the gold-gadolinium mixture. This result was checked not only for the single point in T-ρ parameter space at which the experimental comparison was made, but over a whole region appropriate to the evolution of the wall plasma inside the hohlraum. In fact, we showed that the opacity comparison of mixtures obtained at one point in T-ρ space can be asssumed to hold over a reasonably broad

region around that point. The Au-Cu alloy is a very interesting combination because copper is much easier to mix with gold than any rare earth element and it is easy to work with. In addition we saw that the optimal concentration for Cu was above 60%, a somewhat surprising result since the opacity for pure Cu at 250 eV was only 952 cm^2/g. In fact, we showed that nickel can also be used instead of copper and presents very similar opacity characteristics when mixed with gold, but of course with different mechanical properties.

We also showed that replacing gold by a mixture increases the opacity relatively more at higher hohlraum temperatures.

We have shown that it is essential to have an accurate calculation of the detailed spectra, using for example an STA type of model. Non-LTE effects are not very important at the density around 1 g/cm^3 considered in this paper, although using an effective temperature lower than 250 eV moves the results of the computation closer to the experimental data. Based upon our studies, a mixture of 60% copper and 40% gold should provide a usefully higher overall opacity for laser fusion hohlraums. The higher opacity might allow the designer to use a slightly larger hohlraum, thereby improving the symmetry and/or the coupling efficiency. This copper /gold mixture is an easily made alloy.

Acknowledgements

This work was supported by US DoE. We thank Dr. S.E. Bodner for his continuing interest in this work and for carefully reading the manuscript.

References

[1] T. J. Orzechowski, M. D. Rosen, H. N. Kornblum, J. L. Porter, L. J. Sutter, A. R. Thiessen and R. J. Wallace, *Phys. Rev. Lett.*, **77**, 3545 (1996).

[2] W. A. Lokke and W. H. Grasburger, Lawrence Livermore National Laboratory, Report UCRL-52276 (1977)-unpublished.

[3] A. Bar-Shalom, J. Oreg, W. H. Goldstein, D. Shvarts and A. Zigler, *Phys. Rev. A*, **40**, 3183 (1989).

[4] A. Bar-Shalom, J. Oreg and W. H. Goldstein, in *IVth International Workshop on Radiative Properties of Hot Dense Matter, Sarasota, Fla, 1990*, edited by W. H. Goldstein, C. Hooper, J. C. Gauthier, J. Seely and R. Lee, (World Scientific), p. 163.

[5] A. Bar-Shalom, J. Oreg and W. H. Goldstein, in *Atomic Processes in Plasmas, Portland, Maine, 1991*, edited by E. S. Marmar and J. L. Terry, (AIP), p. 68.

[6] A. Bar-Shalom, J. Oreg, J. F. Seely, U. Feldman, C. M. Brown, B. A. Hammel, R. W. Lee and C. A. Back, *Phys. Rev. E*, **52**, 6686 (1995).

[7] P. T. Springer, D. J. Fields, B. G. Wilson, J. K. Nash, W. H. Goldstein, C. A. Iglesias, F. J. Rogers, J. K. Swenson, M. H. Chen, A. Bar-Shalom and R. E. Stewart, *Phys. Rev. Lett.*, **69**, 3735 (1992).

[8] P. T. Springer, T. S. Perry, D. F. Fields, W. H. Goldstein, B. G. Wilson and R. E. Stewart, in *Atomic Processes in Plasmas, Portland, Maine, 1991*, edited by E. S. Marmar and J. L. Terry, (A I P), p. 78 .

[9] G. Winhart, K. Eidmann, C. A. Iglesias, A. Bar-Shalom, E. Minguez, A. Rickert and S. J. Rose, *J. Quant. Spectrosc. Radiat. Transfer.*, **54**, 437 (1995).

[10] B. L. Henke, E. M. Gullikson and J. C. Davis, *Atom. Dat. & Nuc. Dat. Tables*, **54**, 181 (1993).

[11] M. Busquet, *Phys. Fluids B*, **5**, 4191 (1993).

[12] M. Klapisch and D. Colombant, *Bull. Am. Phys. Soc.*, **41**, 1556 (1996).

[13] A. Bar-Shalom, J. Oreg and M. Klapisch, in *Radiative properties of hot dense matter, Santa Barbara, CA, 1996*, edited by R. W. Lee, to be published in J. Quant. Spectrosc. Radiat. Transfer (1997)

[14] M. Klapisch and A. Bar-Shalom, in *Radiative properties of hot dense matter, Santa Barbara, CA, 1996*, edited by R. W. Lee, to be published in J. Quant. Spectrosc. Radiat. Transfer (1997)

[15] A. Bar-Shalom and M. Klapisch, *Bull. Am. Phys. Soc.*, **41**, 1478 (1996).

[16] L. J. Suter, R. L. Kauffman, C. B. Darrow, A. A. Hauer, H. Kornblum, O. L. Landen, T. J. Orzechowski, D. W. Phillion, J. L. Porter, L. V. Powers, A. Richard, M. D. Rosen, A. R. Thiessen and R. Wallace, *Phys. Plasmas*, **3**, 2057 (1996).

Table Captions

TABLE I. Average charge Z^* for Cu and Gd for two temperatures.

TABLE II. Rosseland mean opacity and energy of the relevant absorption peak for the various elements and mixtures considered in this work, at T_e =250eV and density of 1g/cm^3.

TABLE III. Rosseland mean opacity for pure and mixed elements for an effective ionization temperature T_Z = 243eV taking into account non-LTE effects.

TABLE I.

Element	Z^* (T=150 eV)	Z^* (T=300 eV)
Cu	15.10	19.88
Gd	21.79	31.95

TABLE II.

Element	Rosseland mean (cm^2/g) for pure element	Energy (eV) of absorption peak near 1 keV	Maximum Rosseland mean when mixed with Au	Optimum % of Au
Ag	1844	767	2036	20
Co	1140	983	2169	20
CsI	2056	967	2566	30
Cu	952	1117	2263	30
Gd	1377	1400	2162	50
Mn	1209	866	1913	20
Nd	1509	1200	2475	50
Ni	1118	1083	2291	20
Se	657	1550	1860	50
Sn	1997	850	2280	20

TABLE III.

Element	Rosseland mean (cm^2/g) for pure element.	Percentage change w/r to T_e=250eV.	Maximum Rosseland mean when mixed with Au.
Ag	1983	7.5	2157
Co	1173	2.9	2280
CsI	2075	2.3	2643
Cu	968	1.7	2351
Gd	1426	3.5	2262
Mn	1281	5.9	2029
Nd	1535	1.7	2563
Ni	1144	2.3	2362
Sn	2119	6.1	2400

Figure Captions

FIG. 1 Rosseland mean opacities for mixtures of Au-Gd, Au-Cu, and Au-Ni at a temperature of 250 eV and a total mass density of $1 g/cm^3$. The horizontal axis is the fraction of Au in the mixtures.

FIG. 2 Rosseland mean opacities at a density of $1 g/cm^3$, as a function of T_e. *a*)30%Au-70%Cu. *b*)70%Au-30%Gd. *c*)100%Au.

FIG. 3 Rosseland mean opacities at a temperature of 250eV, as a function of density. *a*)30%Au-70%Cu. *b*)50%Au-50%Gd. *c*)100%Au.

FIG. 4 Frequency dependent opacity of Cu and Gd at T=150eV and $\rho=1 g/cm^3$, along with the corresponding Rosseland weight function $\partial B_\nu / \partial T$.

FIG. 5 Frequency dependent opacity of Cu and Gd at T=300eV and $\rho=1 g/cm^3$, along with the corresponding Rosseland weight function $\partial B_\nu / \partial T$.

FIG.6 Frequency-dependent opacity of CsI+Gd+Ag (see text), which combined with gold give the maximum average Rosseland mean opacity obtained in this study. Note that the minima around 1 keV have been filled up rather thoroughly.

FIG.7 Rosseland mean opacities for a mixture of Au-Gd at T=243 eV and T=250 eV. This data is compared with ref.[1] experimental data and XSN simulations.

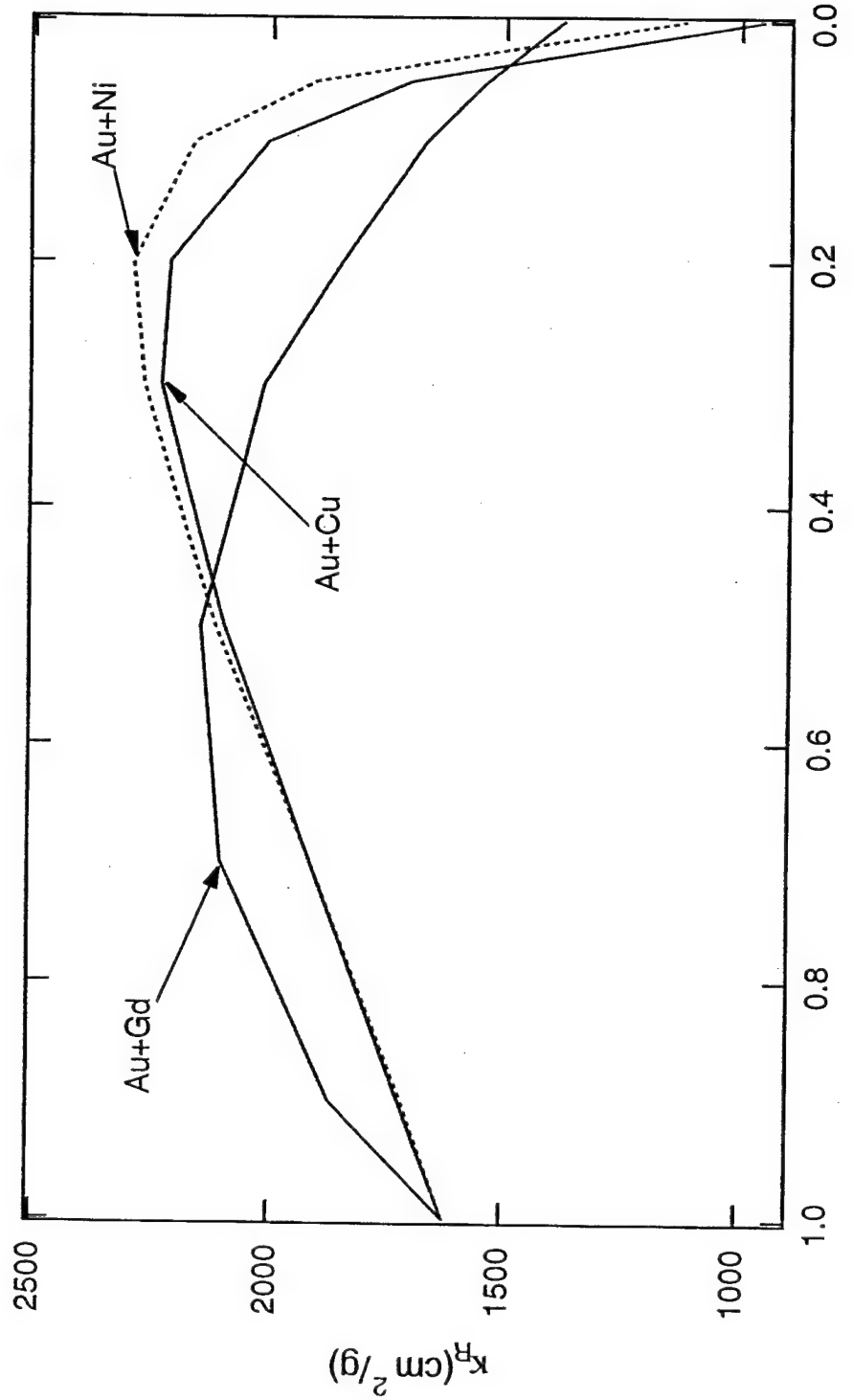
2500
2000
1500
1000
$\kappa_R(cm^2/g)$
1.0
0.8
0.6
0.4
0.2
0.0
Fraction of Au
Au+Gd
Au+Cu
Au+Ni

Figure 1

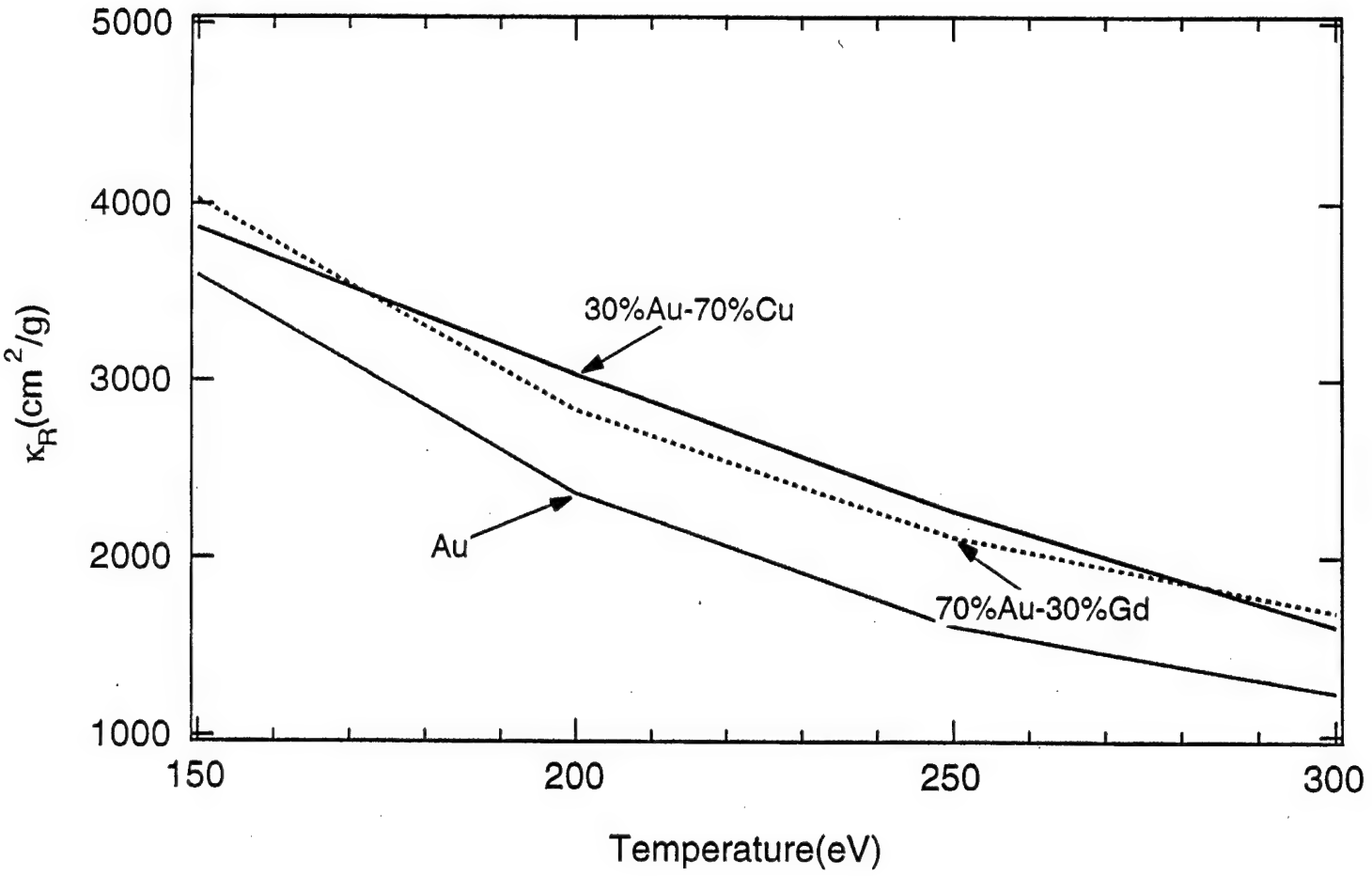
5000
4000
3000
2000
1000
150
200
250
300
$\kappa_R(cm^2/g)$
Temperature(eV)
30%Au-70%Cu
Au
70%Au-30%Gd

Figure 2

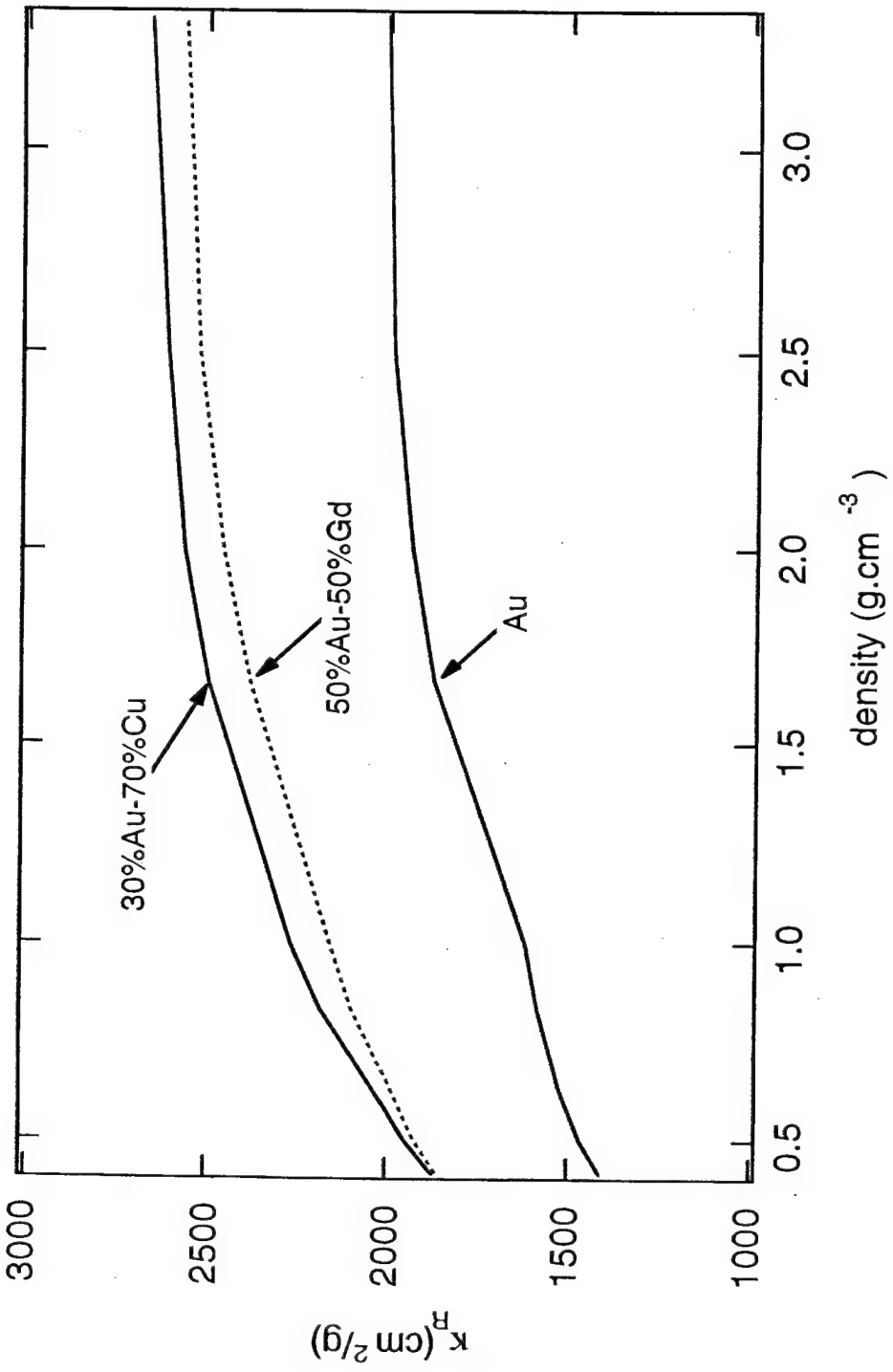
3000
2500
2000
1500
1000
0.5
1.0
1.5
2.0
2.5
3.0
density (g.cm -3)
κR(cm2/g)
30%Au-70%Cu
50%Au-50%Gd
Au

Figure 3

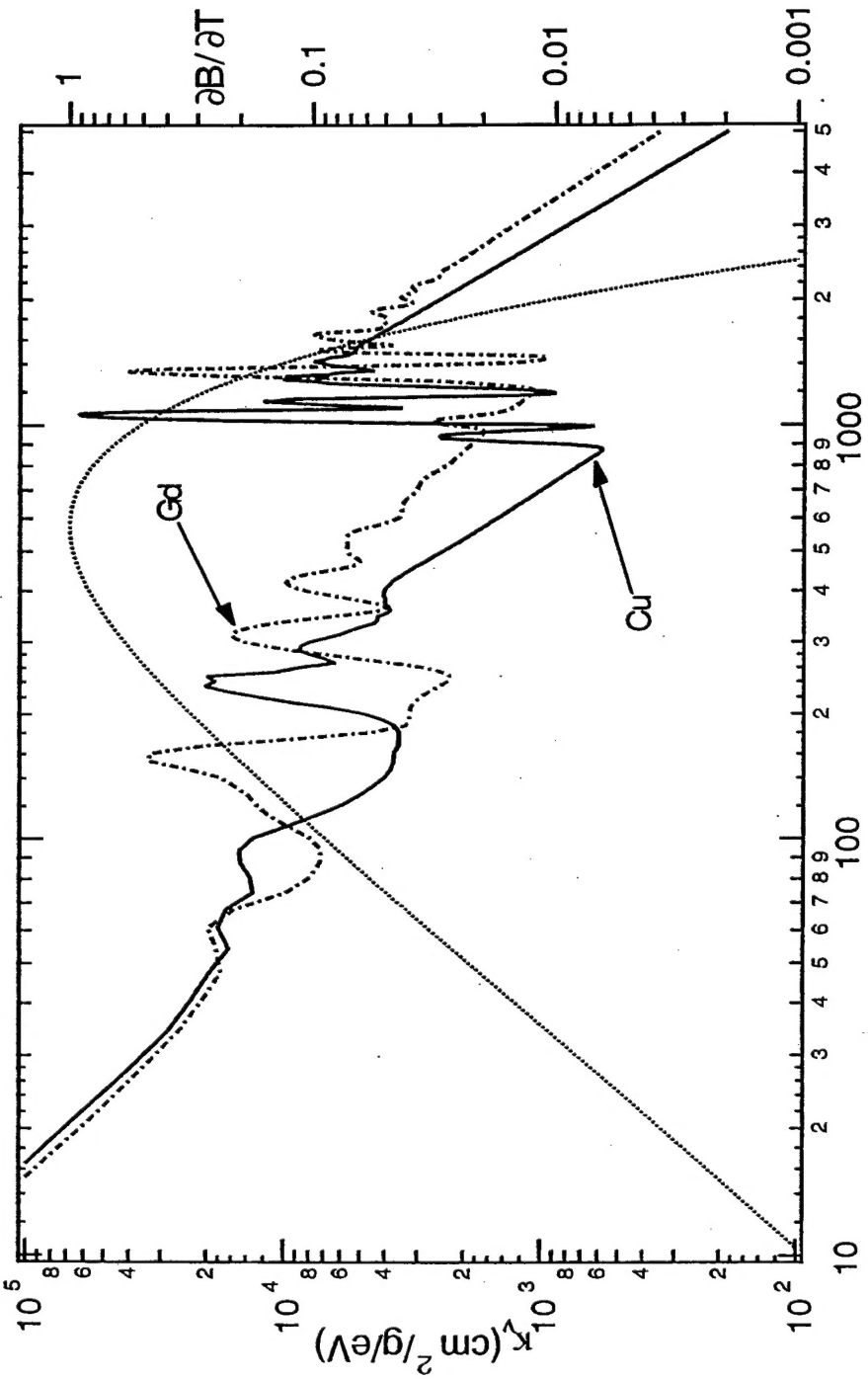
1
∂B/∂T
0.1
0.01
0.001
Gd
Cu
10^5
10^4
10^3
10^2
k_γ(cm^2/g/eV)
10
100
1000
Photon energy(eV)

Figure 4

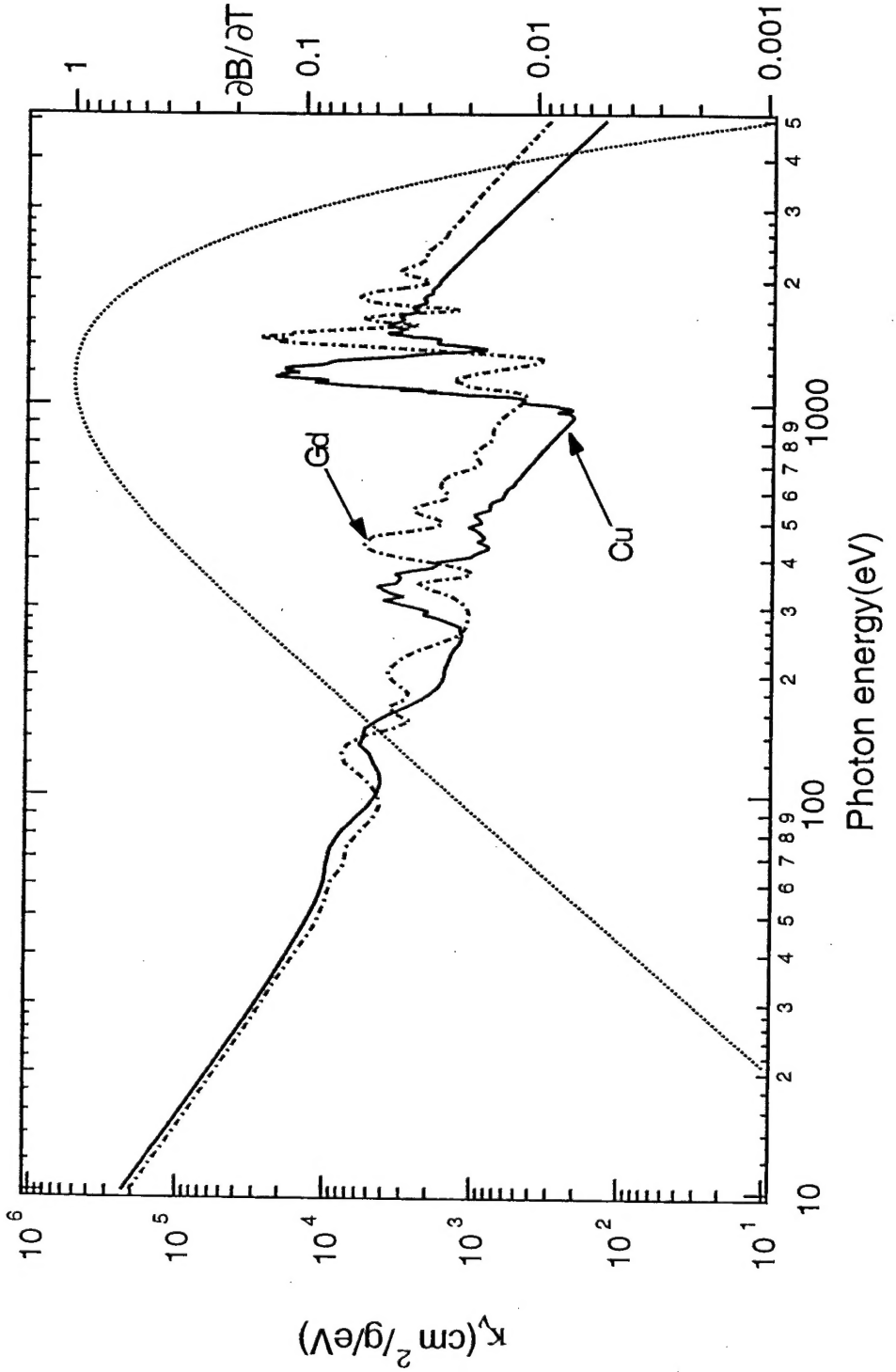
1
∂B/∂T
0.1
0.01
0.001
Gd
Cu
10^6
10^5
10^4
10^3
10^2
10^1
10
100
1000
Photon energy(eV)
κ_γ(cm^2/g/eV)

Figure 5

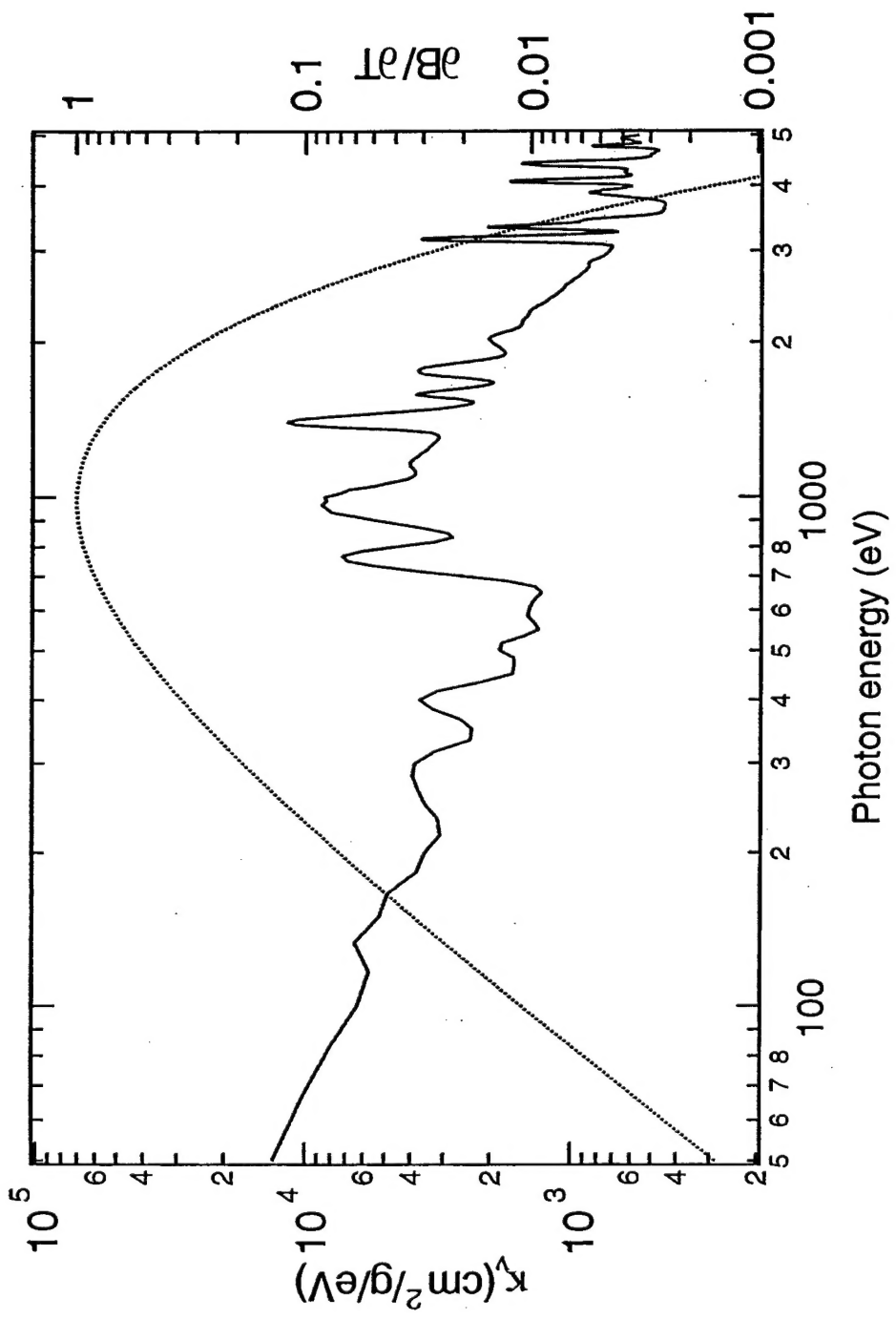
κ_ν(cm^2/g/eV)
10^5
10^4
10^3
100
1000
Photon energy (eV)
1
0.1
0.01
0.001
$\partial B/\partial T$

Figure 6

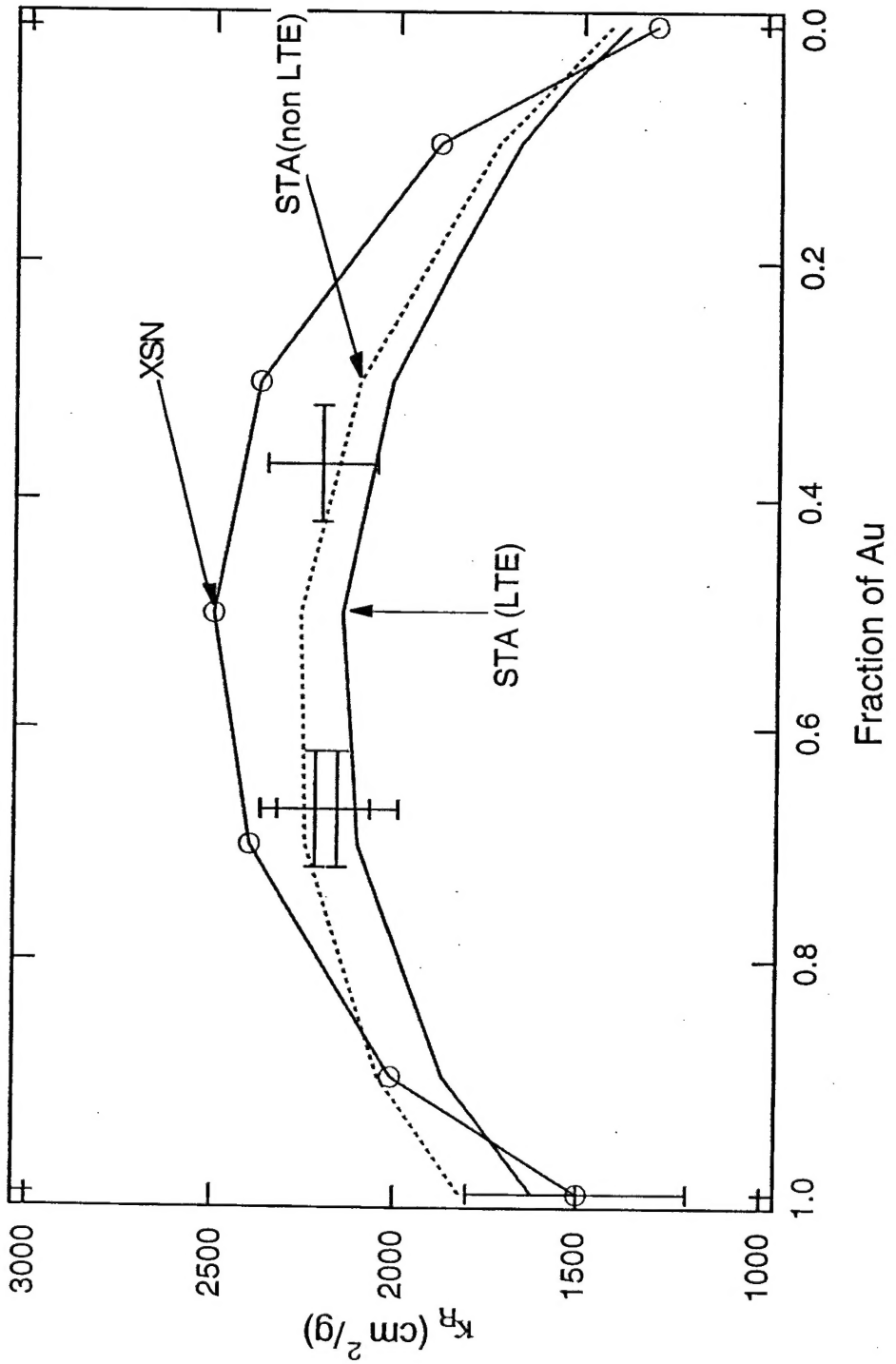
XSN
STA(non LTE)
STA (LTE)
κ_R (cm^2/g)
3000
2500
2000
1500
1000
1.0
0.8
0.6
0.4
0.2
0.0
Fraction of Au

Figure 7